Journal of Pharmacokinetics and Biopharmaceutics, Vol. 10, No. 3, 1982

Physiologically Based Pharmacokinetics of Drug-Drug Interaction: A Study of Tolbutamide-Sulfonamide Interaction in Rats

Osamu Sugita[1], Yasufumi Sawada[1], Yuichi Sugiyama[1], Tatsuji Iga[1], and Manabu Hanano[1,2]

Received September 29, 1981—Final April 5, 1982

A blood flow rate-limited pharmacokinetic model was developed to study the effect of sulfonamide on the plasma elimination and tissue distribution of ^{14}C-tolbutamide (TB) in rats. The sulfonamides (SA) used were sulfaphenazole (SP), sulfadimethoxine (SDM), and sulfamethoxazole (SMZ). The tissue-to-plasma partition coefficients (Kp) of all tissues studied, i.e., lung, liver, heart, kidney, spleen, G.I. tract, pancreas, brain, muscle, adipose tissue, and skin, increased in the presence of SA, but except for brain, liver, and spleen, the tissue-to-plasma unbound concentration ratio (Kp, f) of other tissues did not show a significant alteration. This suggested that the tissue binding of TB is not affected by SA and that the increase of Kp is due mainly to the displacement of plasma protein-bound TB by SA. The concentrations of TB in several tissues and plasma were predicted by a physiologically based pharmacokinetic model using in vitro plasma binding and metabolic parameters, the plasma-to-blood concentration ratio and the tissue-to-plasma unbound concentration ratios having been determined from both the tissue and plasma concentrations of TB at the β-phase after intravenous administration of TB and the plasma free fraction. The predicted concentration curves of TB in each tissue and in plasma showed good agreement with the observed values except for the brain, for which the predicted concentrations were lower than the observed values in the early time period. In the SP- and SDM-treated rats, the predicted free concentration of TB in the target organ, the pancreas, at 6 h was six times higher than that of the control rats. From these findings, it is suggested that physiologically based pharmacokinetic analysis could be generally useful to predict approximate plasma and tissue concentrations of a drug in the presence of drug-drug interaction.

KEY WORDS: drug-drug interaction; tolbutamide-sulfonamide interaction; sulfaphenazole; sulfadimethoxine; sulfamethoxazole; physiological pharmacokinetics.

This study was supported by a grant-in-aid for Scientific Research provided by the Ministry of Education, Science and Culture of Japan.

[1]Faculty of Pharmaceutical Sciences, University of Tokyo, Hongo, Bunkyo-ku, Tokyo 113, Japan.

[2]Correspondence to Dr. Manabu Hanano.

0090-466X/82/0600-0297$03.00/0

INTRODUCTION

The recent development of anatomically and physiologically realistic pharmacokinetic models for drug disposition based on actual organ blood or plasma flows and physiological volumes (1–3) has made it possible to predict, in principle, the drug concentration in any tissue at any time and to provide considerable insight into drug dynamics. A further advantage of these models is that the drug disposition in disease states may be simulated by altering estimates of organ blood flow (4, 5), metabolism of the drug, urinary or biliary clearance of the drug (6), or plasma and tissue binding of the drug. Furthermore, the most important application is interspecies scale-up, where the large data base required to develop a physiological pharmacokinetic model may be determined in a laboratory animal and scaled up to apply to humans. This approach has been applied successfully to predict the disposition of thiopental (7), methotrexate (8), 1-β-D-arabinofuranosylcytosine (9), lidocaine (4), sulfobromophthalein (10), adriamycin (11), and digoxin (12). However, little work has been reported on the effect of drug-drug interaction on plasma protein binding, excretion, metabolism, and tissue distribution as determined by physiologically based pharmacokinetic analysis (13,14). The interaction of tolbutamide (TB), a sulfonylurea derivative, with a second drug, e.g., sulfonamide (SA), has been extensively studied, and two possible mechanisms have been suggested, i.e., displacement of plasma protein-bound drug and metabolic inhibition (15–21). Recently, the prediction of TB–SA interaction from the *in vitro* unbound intrinsic clearance was studied by comparing the total body clearance (CL_{tot}) obtained from *in vivo* and *in vitro* experiments in rats (22). A comparatively good agreement was observed between the *in vivo* CL_{tot} and that calculated from both *in vitro* plasma binding and metabolic parameters. However, the effects of SA on the tissue distribution of TB have not been investigated yet.

The purpose of this study was to develop a physiologically based pharmacokinetic model for the drug interaction of TB with SA and to predict the unbound concentration versus time profile of TB in the target organ, the pancreas, in the presence and absence of SA. Sulfonamides employed were sulfaphenazole (SP), sulfadimethoxine (SDM), and sulfamethoxazole (SMZ).

MODEL DEVELOPMENT

A physiologically based pharmacokinetic model for the distribution, disposition, and excretion of TB in rats is shown in Fig. 1. The model consists of eleven tissues and blood compartments, which represent real

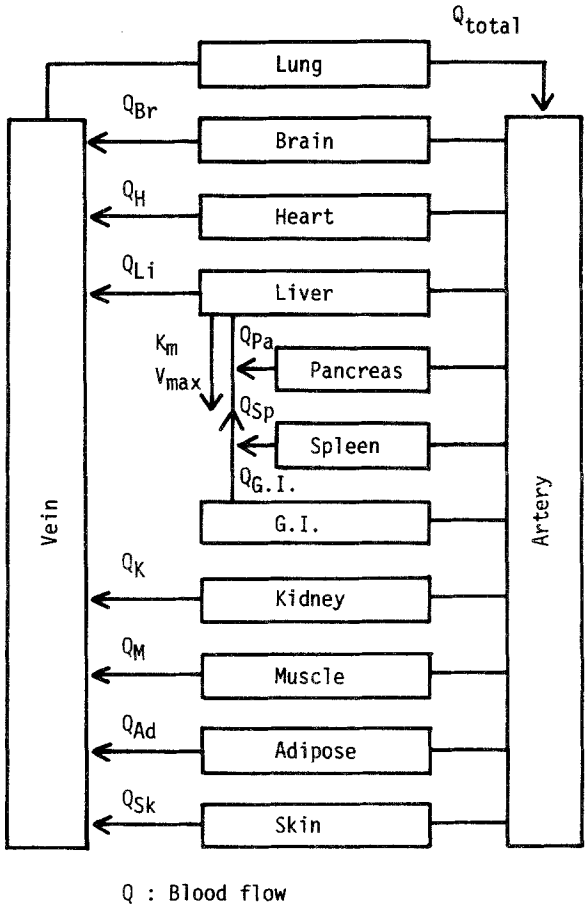

Fig. 1. Pharmacokinetic model for the disposition of tolbutamide (TB) in rats.

organs or anatomic tissue regions in the body. This model assumes that (a) each tissue acts as a well-stirred compartment, (b) intercompartmental transport occurs by blood flow, (c) distribution of TB is a blood flow-limited and linear process, (d) only free TB is available for tissue distribution, (e) elimination of TB occurs only by the metabolism of free TB in the liver and renal clearance is negligible (21), and (f) TB binds to only one population of sites of plasma proteins. The plasma free fraction (f_p) is expressed by a modified Scatchard equation,

$$f_p = \frac{C_{p,f}}{C_{p,f} + [n(p)C_{p,f}/(K_{d,app} + C_{p,f})]} \quad (1)$$

$K_{d,app}$ is given by the following equation:

$$K_{d,app} = K_d\left(1+\frac{I_f}{K_I}\right) \tag{2}$$

where I_f and K_I are the free concentration of SA and the inhibitor constant of SA for TB plasma protein binding (dissociation constant for SA), respectively, and $C_{p,f}$ is the plasma unbound concentration of TB. The oxidative metabolic rate of TB follows the Michaelis–Menten equation:

$$v = \frac{V_{\max}C_{p,f}}{(K_{m,app}+C_{p,f})} \tag{3}$$

$K_{m,app}$ is given by the following equation:

$$K_{m,app} = K_m\left(1+\frac{I_f}{K_i}\right) \tag{4}$$

where K_i is the inhibitor constant of SA for oxidative metabolism of TB. The assumptions that the plasma protein binding and microsomal oxidation of TB were competitively inhibited by SA were validated from the *in vitro* studies in a previous paper (22).

The mass balance–blood flow equations were written for the concentration in each compartment shown in Fig. 1. The complete set of differential equations is given in Appendix II and was solved numerically by the Runge–Kutta–Marson method using a Hitachi M200-H digital computer (23). Physiological constants used in the simulation for a 280 g rat are listed in Table I. Tissue volumes except for muscle and blood were determined experimentally from the wet tissue weight by assuming a density of 1.0 for each tissue. The muscle volume was assumed to be half of the body weight (24). The blood volume was calculated according to Bischoff *et al.* (8) as follows:

$$V_{\text{plasma}} = 44 \times (\text{body weight, kg})^{0.99} \tag{5}$$

$$V_{\text{blood}} = V_{\text{plasma}}/(1-H_t) \tag{6}$$

where H_t is the hematocrit value, which was determined to be 0.41 in this study. The volume ratio of arterial to venous blood was assumed to be the same as that of humans, i.e., 0.5 (4). The blood flow rate of the lung was assumed to be the same as that of an artery or vein. Blood flow rates of other tissues or organs were obtained from the literature (25–27) (see Table I). Various parameters for plasma protein binding and metabolism used in the simulation were obtained from *in vitro* studies reported previously (22) and are summarized in Table II. The tissue-to-plasma unbound concentration ratios (Kp, f) used in the simulation are listed in Table IV (see Results).

Table I. Physiological Constants for the Distribution of Tolbutamide in Rats[a]

Tissue	Blood flow (ml/min)	Volume[b] (ml)	Tissue	Blood flow (ml/min)	Volume[b] (ml)
Artery	51.9[c]	7.0	Kidney	12.8[f]	2.2
Vein	51.9[c]	14.1	Muscle	7.6[f]	140.0
G.I. tract	12.3[d]	12.4	Skin	5.0[f]	49.0
Lung	51.9[e]	1.3	Adipose tissue	0.4[g]	11.2
Brain	3.2[d]	1.3	Pancreas	1.0[d]	1.0
Heart	6.4[d]	1.2	Spleen	1.0[d]	1.0
Liver	16.5[f]	12.4			

[a] Based on a 280-g rat.
[b] Determined experimentally from the wet tissue weight by assuming a density of 1.0 for each tissue for muscle and blood volume (artery and vein) (see text under model development).
[c] $Q_{Br} + Q_H + Q_{Li} + Q_K + Q_M + Q_{Sk} + Q_{Ad}$.
[d] Sasaki and Wagner (25).
[e] Assumed to be the same as those of artery and vein.
[f] Dedrick *et al.* (26).
[g] Lutz *et al.* (27).

MATERIALS AND METHODS

Sodium tolbutamide (TB), sodium sulfadimethoxine (SDM), and sodium sulfamethoxazole (SMZ) were kindly supplied by Japan Hext, Tokyo, Japan, Daiichi Pharm. Co., Tokyo, Japan, and Shionogi Co., Ltd.,

Table II. Parameters for Plasma Protein Binding, Plasma-to-Blood Concentration Ratio, and Metabolism of Tolbutamide in Rats[a]

Parameters	Control	+SP[b]	+SDM[c]	+SMZ[d]
Free concentration of SA[e] in plasma, I_f (mM)		0.77	0.69	1.67
Plasma-to-blood concentration ratio, s	1.33	1.27	1.23	1.37
Plasma protein binding[f]				
Binding capacity, $n(p)$ (mM)	1.13	1.13	1.13	1.13
Inhibitor constant of SA[e], K_I (mM)		0.325	0.243	2.929
Apparent dissociation constant, $K_{d,app}$ (mM)	0.300	1.010	1.149	0.471
Metabolism in liver				
Maximum velocity, V_{max} (μmol TB metabolized/min/12.4 g liver)	1.44	1.44	1.44	1.44
Inhibitor constant of SA[e], K_i (mM)		0.30	0.24	6.69
Apparent Michaelis constant, $K_{m,app}$ (mM)	0.96	3.42	3.75	1.20

[a] Parameters obtained from a previous paper (22), corresponding to those at the steady-state concentration of sulfonamides (500 μg/ml).
[b] Sulfaphenazole.
[c] Sulfadimethoxine.
[d] Sulfamethoxazole.
[e] Sulfonamides.
[f] Binding experiments were performed by the ultrafiltration method using heparinized plasma (22).

Osaka, Japan, respectively. Sulfaphenozole (SP) was obtained from Dainippon Pharm. Co., Tokyo, Japan. ^{14}C-carbonyl TB (48.09 mCi/mmol) was purchased from New England Nuclear Co., Boston, Mass., and found to be at least 98–99% pure by thin-layer chromatography. All other reagents were commercial products of analytical grade.

Animal Experiments

Adult male Wistar rats (Nihon Seibutsu Zairyo, Tokyo, Japan) weighing 260–280 g were used. Under light ether anesthesia, the femoral vein and artery were cannulated with PE-10 and PE-50 polyethylene tubing, respectively. Cannulated rats were kept in restraining cages with water under normal housing conditions prior to the experiments. After loading doses of 160, 200, and 200 mg/kg SP, SDM, and SMZ, respectively, doses of 50.0, 41.3, and 41.3 mg/kg per h, respectively, were infused through the femoral vein cannula for 6 h and 50 min with a constant rate infusion pump (Natsume Seisakusho Co., Model KN, type 12H, Tokyo, Japan); with these dosages, steady-state concentrations of SA (500 μg/ml) were obtained within 20 and 35 min after the beginning of the infusion. The control rats were given physiological saline instead of SA. At 50 min after the initiation of infusion, the rats were given 80 mg/kg of TB containing 3.33 μCi/kg of ^{14}C-TB in physiological saline through the other femoral veing cannula. For the infusion study of TB, a loading dose of 40.79 mg/kg TB followed by a constant rate infusion of 15.43 mg/kg per h, was administered through the femoral vein cannular for 4 h as described before. The steady-state concentration of TB (approximately 200 μg/ml) was obtained within 1 h after the initiation of infusion. The body temperature was kept at 37°C by means of a heat lamp. After removal of blood samples, the animals were sacrificed at 1, 2, 4, and 6 h after TB administration for the bolus study, and at 4 h for the infusion study, by an injection of saturated KCl solution into the carotid artery. The brain, heart, lung, liver, kidney, spleen, pancreas, G.I. tract, adipose tissue, muscle, skin, thymus, bone marrow, testis, submaxillary gland, and eyeball were quickly excised, rinsed well with cold saline, blotted, and weighed. The wet weights of all these tissues were not altered in the presence of SA. Lymph was collected through a thoracic duct cannula. All tissues, plasma, and lymph were stored at −20°C until study.

The separation of the metabolites from TB was carried out according to Shibasaki *et al.* (19) as described in a previous paper (22). Briefly, tissue samples except for skin were homogenized with a threefold excess volume of 0.5 M phosphate buffer (pH 5.0) in a Teflon-glass homogenizer. Four ml of each homogenate and 50 μl of plasma or lymph sample were shaken

for 30 min and then extracted twice with 6 ml of *n*-heptane-chloroform (4 : 1 v/v). The extracts were combined and shaken with 1 ml of 0.5 N NaOH for 15 min and the aqueous phase was used for the determination of TB. The percent recoveries after the extraction of TB from plasma, lymph, lung, brain, heart, liver, pancreas, spleen, G.I. tract, kidney, muscle, and adipose tissue were 77, 77, 51, 38, 44, 61, 55, 49, 54, and 60%, respectively. The concentration of ^{14}C-labeled TB was determined in an Aloka Tri-Carb counter (Aloka Instruments Co., Tokyo, Japan) after 0.5 ml of the aqueous phase had been placed in a scintillation vial containing 0.5 ml of 0.5 N HCl and 10 ml of scintillation fluid (0.1 g of POPOP, 4.0 g of PPO, and 500 ml of Triton X-100/liter of toluene). Skin was oxidized to $^{14}CO_2$ in a Packard sample oxidizer (Packard Instruments Corp., Downers Grove, Ill.; Model 306), and then the radioactivity was determined as described before.

Statistical Analysis

All means are presented with their standard error (the mean ± SE). Statistical analysis was performed by the use of Student's *t*-test with $p = 0.05$ as the minimal level of significance.

RESULTS

Tissue-to-Plasma Partition Coefficients (*Kp*) of TB

Tissue-to-plasma partition coefficients (*Kp*) at 6 h after intravenous bolus administration of TB in the presence and absence of SA, and those obtained from the steady-state concentration with a constant infusion of TB, are listed in Table III. The *Kp* values of all tissues studied significantly increased in the presence of SP and SDM, while in the presence of SMZ, the *Kp* values of seven tissues, i.e., brain, heart, liver, spleen, G.I. tract, muscle and skin, significantly increased. A representative relationship between the *Kp* values in the presence and those in the absence of SP is shown in Fig. 2.

The free fractions (f_p) in the plasma concentrations of TB were calculated using the binding parameters in Table II, and are listed in Table IV. The f_p significantly increased both in the presence of SA and at the higher TB concentration in the steady state (200 μg/ml) as compared with the control. The tissue-to-plasma unbound concentration ratios (Kp, f) were calculated by the following equation and are also listed in Table IV:

$$Kp, f = \frac{C_t}{C_{p,f}} = \frac{Kp}{f_p} \tag{7}$$

Table III. Tissue-to-Plasma Partition Coefficients (Kp) of Tolbutamide in Rats[a]

Tissue	Control[b]	+Sulfonamides			Steady-state[c]
		SP[b]	SDM[b]	SMZ[b]	
Brain	0.037 ± 0.003	0.210 ± 0.032[d]	0.257 ± 0.026[d]	0.143 ± 0.019[d]	0.097 ± 0.009[d]
Heart	0.180 ± 0.035	0.427 ± 0.062[e]	0.380 ± 0.015[d]	0.310 ± 0.020[e]	0.267 ± 0.038
Lung	0.243 ± 0.020	0.520 ± 0.076[e]	0.453 ± 0.064[d]	0.297 ± 0.050	0.250 ± 0.052
Liver	0.130 ± 0.000	0.303 ± 0.032[d]	0.410 ± 0.056[d]	0.320 ± 0.035[d]	0.303 ± 0.046[e]
Kidney	0.127 ± 0.009	0.270 ± 0.046[e]	0.330 ± 0.030[d]	0.207 ± 0.039	0.220 ± 0.029[e]
Spleen	0.097 ± 0.009	0.303 ± 0.022[e]	0.327 ± 0.013[d]	0.173 ± 0.019[e]	0.193 ± 0.039
Pancreas	0.140 ± 0.020	0.280 ± 0.049[d]	0.277 ± 0.026[e]	0.190 ± 0.023	0.293 ± 0.055
G.I. tract	0.077 ± 0.009	0.223 ± 0.023[e]	0.223 ± 0.022[d]	0.163 ± 0.023[e]	0.117 ± 0.023
Adipose tissue	0.110 ± 0.015	0.247 ± 0.054[d]	0.217 ± 0.022[e]	0.133 ± 0.026	0.130 ± 0.023
Muscle	0.080 ± 0.000	0.230 ± 0.035[d]	0.230 ± 0.015[d]	0.133 ± 0.019[e]	0.130 ± 0.006[e]
Skin	0.187 ± 0.018	0.340 ± 0.046[d]	0.347 ± 0.024[d]	0.287 ± 0.038	0.223 ± 0.026
Lymph	n.d.[f]	n.d.	n.d.	n.d.	0.470 ± 0.010

[a] Results are given as the means ± SE of three rats.
[b] At 6 h after bolus injection of tolbutamide. SP, sulfaphenazole; SDM, sulfadimethoxine; SMZ, sulfamethoxazole (see Methods).
[c] From the constant infusion studies (see Methods).
[d] Significantly different ($p < 0.01$) from the control.
[e] Significantly different ($p < 0.05$) from the control.
[f] Not determined.

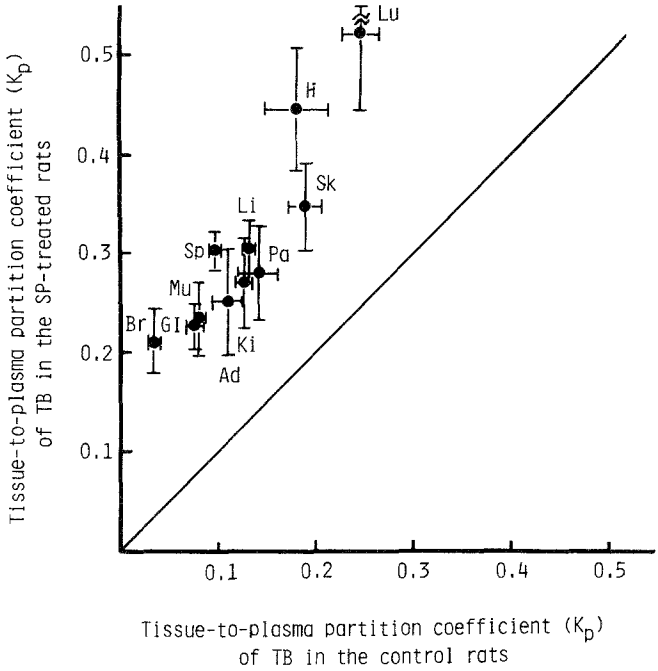

Fig. 2. The relationship between the tissue-to-plasma partition coefficients (*Kp*) of tolbutamide (TB) in the presence and those in the absence of sulfonamides (SA). Abbreviation Li, Ki, GI, Lu, H, M, Br, Pa, Sp, Ad, and Sk denote liver, kidney, gastrointestinal tract, lung, heart, muscle, brain, pancreas, spleen, adipose tissue, and skin, respectively. The line shows a positive correlation ($r = 1.000$).

where C_t is the total tissue concentration of TB and $C_{p,f}$ is the plasma unbound concentration of TB. Significant increases of Kp,f were seen in the brain and spleen of the SP- and SDM-treated rats, and in the brain and liver of the SMZ-treated rats, but those of other tissues did not show a significant alteration. The Kp,f of the steady state from the constant infusion studies also did not show a significant alteration except for the brain and liver, which showed significant increases. A representative relationship between the Kp,f values in the presence and those in the absence of SP is shown in Fig. 3, and a good correlation was observed except for the brain.

Predicted Time Course of TB Concentration in Plasma and Tissues

The *Kp* values determined were used for the physiologically based pharmacokinetic simulation after correction by the method of Chen and

Table IV. Tissue-to-Plasma Unbound Concentration Ratio (Kp, f) of Tolbutamide in Rats[a]

Tissue	Control[d]	+Sulfonammides			Steady-state[e]
		SP[d]	SDM[d]	SMZ[d]	
C_p (μg/ml)[b]	58.1 ± 4.8	146.5 ± 9.8[f]	85.8 ± 3.5[f]	42.1 ± 7.1[f]	207.1 ± 9.3[f]
f_p[c]	0.236 ± 0.003	0.530 ± 0.007[f]	0.515 ± 0.022[f]	0.312 ± 0.005[f]	0.329 ± 0.006[f]
Brain	0.155 ± 0.013	0.397 ± 0.062[g]	0.501 ± 0.055[f]	0.459 ± 0.060[f]	0.295 ± 0.032[g]
Heart	0.767 ± 0.150	0.807 ± 0.122	0.740 ± 0.058	0.994 ± 0.077	0.830 ± 0.141
Lung	1.092 ± 0.081	0.983 ± 0.151	0.990 ± 0.039	0.954 ± 0.164	0.761 ± 0.167
Liver	0.551 ± 0.006	0.571 ± 0.057	0.797 ± 0.098	1.022 ± 0.099[f]	0.926 ± 0.158[g]
Kidney	0.537 ± 0.041	0.511 ± 0.092	0.640 ± 0.048	0.665 ± 0.132	0.670 ± 0.093
Spleen	0.410 ± 0.018	0.573 ± 0.047[g]	0.637 ± 0.002[f]	0.538 ± 0.074	0.587 ± 0.117
Pancreas	0.595 ± 0.090	0.529 ± 0.095	0.535 ± 0.032	0.593 ± 0.094	0.893 ± 0.175
G.I. tract	0.324 ± 0.036	0.423 ± 0.050	0.431 ± 0.025	0.524 ± 0.074	0.359 ± 0.077
Adipose tissue	0.465 ± 0.064	0.466 ± 0.101	0.426 ± 0.064	0.430 ± 0.091	0.393 ± 0.067
Muscle	0.339 ± 0.004	0.435 ± 0.070	0.449 ± 0.040	0.427 ± 0.060	0.398 ± 0.025
Skin	0.784 ± 0.079	0.643 ± 0.091	0.679 ± 0.072	0.924 ± 0.128	0.679 ± 0.088

[a] Results are given as the means ± SE of three rats.
[b] Plasma concentration of tolbutamide.
[c] Plasma free fraction of tolbutamide.
[d] At 6 h after bolus injection of tolbutamide. SP, sulfaphenazole; SDM, sulfadimethoxine; SMZ, sulfamethoxazole (see Methods).
[e] From the constant infusion studies (see Methods).
[f] Significantly different ($p < 0.01$) from the control.
[g] Significantly different ($p < 0.05$) from the control.

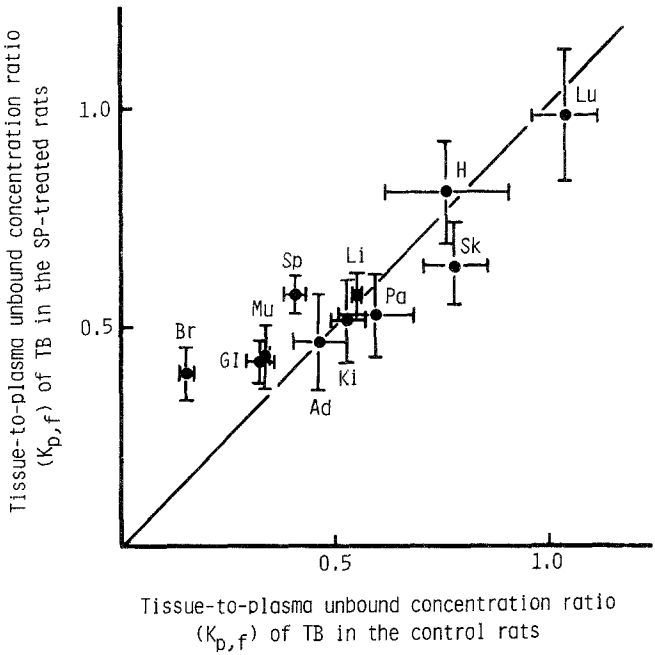

Fig. 3. The relationship between the tissue-to-plasma unbound concentration ratios (Kp, f) of tolbutamide (TB) in the presence and those in the absence of sulfonamides (SA). Abbreviations are the same as those in Fig. 2. The line shows a positive correlation ($r = 1.000$).

Gross (28). The sum of the distribution volumes (ΣKpV) of thymus, bone marrow, testis, and eyeball was determined to be 1.21 ml/kg and was negligible in comparison with that of the 11 tissues shown in Fig. 1. Thus, we ignored these tissues in the model development.

Thirteen differential equations (see Appendix II) were solved simultaneously by the Runge–Kutta–Marson method using the parameters listed in Tables I, II, and IV. The predicted time courses of TB concentration in plasma after intravenous administration of 80 mg/kg of TB in the presence and absence of SA are shown in Fig. 4. Fairly good agreements were obtained between the predicted and observed plasma concentrations of TB in the control (panel a), SP- (panel b), and SDM-treated rats (panel c), while in the SMZ-treated rats, the predicted values were higher than those observed (panel d). Figure 5 shows the predicted and observed concentrations of TB in the target organ, the pancreas (panel a), as well as in the muscle (panel b), brain (panel c), and liver (panel d) after intravenous bolus administration of 80 mg/kg TB to the control and SP-

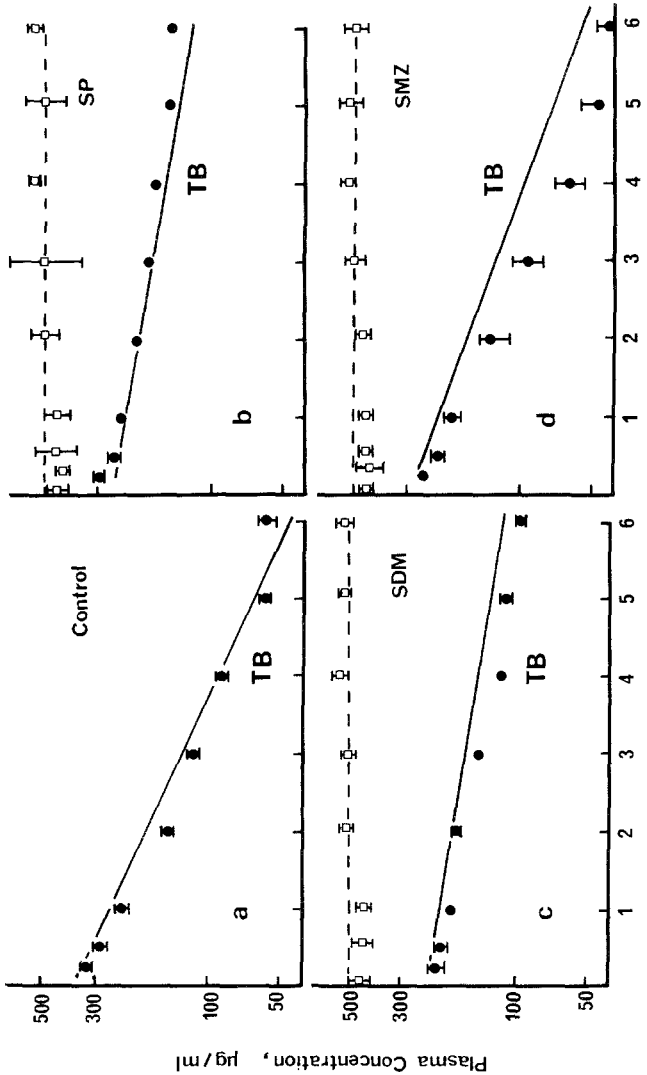

Fig. 4. Predicted and observed log plasma concentration of tolbutamide (TB) after intravenous administration of 80 mg/kg in the presence and absence of sulfonamides (SA) in rats. Each point and vertical bar represent the mean ± SE of three rats. (a) Control (without SA), (b) with sulfaphenazole (SP) ($C_{ss} = 493.4 \pm 33.3$ µg/ml; $n = 3$), (c) with sulfadimethoxine (SDM) (516.8 ± 5.8; $n = 3$), and (d) with sulfamethoxisazole (SMZ) (493.4 ± 5.7; $n = 3$). Key: (●) plasma concentration of TB; (□) plasma concentration of SA; (———) predicted concentration of TB; (- - -) mean concentration of SA for 6 h with a constant infusion (see Methods).

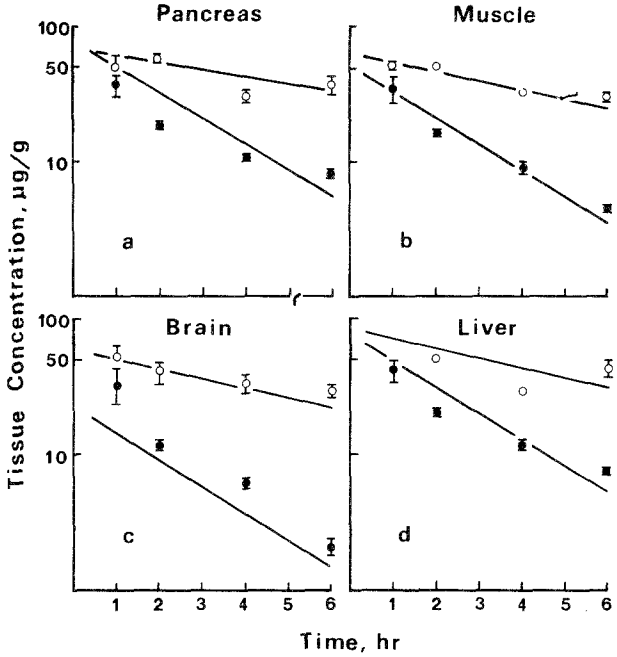

Fig. 5. Predicted and observed log tissue concentration of tolbutamide (TB) after intravenous administration of 80 mg/kg in the presence and absence of sulfaphenazole (SP) in rats. (a) Pancreas, (b) muscle, (c) brain, and (d) liver. Key: (●) tissue concentration of TB without SA; (○) tissue concentration of TB with SA; (———) predicted concentration of TB (see Methods).

treated rats. The predicted TB concentrations of other tissues at 6 h after administration in the control and SP-treated rats are now shown in the figures of this paper, but good agreements were again observed. Equally good agreements were observed in the SDM- and SMZ-treated rats (unpublished data). Most model predictions agreed reasonably well with observed values in both the control and SP-treated rats, while the predicted time course of brain TB concentrations in the control rats was lower than the observed values. Although the determination of the unbound TB concentration in the pancreatic vein is extremely difficult, the pharmacological and toxicological effects of TB are thought to be related to the unbound TB concentration. In this study we attempted to predict the unbound concentration in the pancreatic vein in the presence and absence of SA. The predicted pancreatic venous unbound TB concentrations in the presence of both SP and SDM were very much higher than those of the control and SMZ-treated rats (Fig. 6).

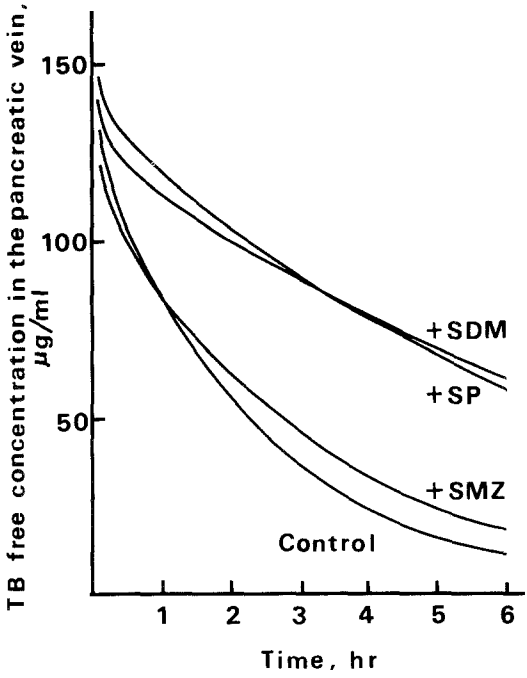

Fig. 6. Predicted free concentration curves of tolbutamide (TB) in the pancreatic vein after intravenous administration of 80 mg/kg in the presence and absence of sulfonamides (SA). SP, sulfaphenazole; SDM, sulfadimethoxine; SMZ, sulfamethoxazole.

DISCUSSION

When the metabolism is the rate-determining step of the hepatic extraction, the total body clearance (CL_{tot}) and the volume of distribution at the steady state (V_{ss}) can be expressed by Eqs. (8) and (9), respectively (29):

$$CL_{tot} \simeq f_p \cdot CL_{int} \tag{8}$$

$$V_{ss} \simeq \frac{V_B}{s} + \sum_j f_p \cdot Kp, f_j \cdot V_j \tag{9}$$

where f_p, CL_{int}, s, and Kp, f are the plasma free fraction, the intrinsic clearance of unbound drug, the plasma-to-blood concentration ratio, and the tissue-to-plasma unbound concentration ratio, respectively. The subscript j represents all tissues studied. The plasma half-life ($t_{1/2}$) can be

expressed by

$$t_{1/2} = \frac{0.693 \cdot Vd}{CL_{\text{tot}}} \tag{10}$$

Combining Eqs. (8), (9), and (10) gives

$$t_{1/2} = 0.693\left[\frac{V_B}{s \cdot f_p \cdot CL_{\text{int}}} + \left(\sum_j Kp, f_j \cdot V_j \Big/ CL_{\text{int}}\right)\right] \tag{11}$$

The relationship of Eq. (11) shows that both the changes of s, f_p, and Kp, f due to the displacement by the second drug and the change of CL_{int} due to the metabolic inhibitor or induction may affect $t_{1/2}$. The effects of SA on f_p and CL_{int} of *TB* were previously reported (20, 22), but the effect of SA on the tissue distribution of TB has not previously been investigated.

Though the Kp values for most of the tissues studied in the presence of SA and at a higher steady-state TB concentration (200 μg/ml) than those of the control significantly increased, the Kp, f values calculated by Eq. (1) did not show an alteration (Tables III and IV). The tissue binding of TB did not depend on the plasma TB concentration and was not decreased in the presence of SA, while the plasma protein binding showed a nonlinearity and was decreased in the presence of SA (22). From these findings, it was suggested that the increase in Kp might be mainly explained by the alteration of the plasma protein binding of TB. As previously reported, no displacement of tissue-bound thiopental by SDM was seen in rat muscle, liver, and adipose tissue homogenates (30). Moreover, the tissue binding of TB was not significantly influenced by phenylbutazone in rabbit muscle homogenates (31). Wardell (32) also reported that phenylbutazone did not significantly affect the tissue binding of SDM in rat muscle, liver, and kidney homogenates. Thus, the increase in Vd_{ss} of TB in the presence of SA (22) might be explained by the unchanged tissue binding of TB and the increase in the plasma free fraction of TB caused by the displacement of plasma-bound TB by SA. However, in sheep, Thiessen and Rowland (20) reported that though the plasma free fraction of TB increased, Vd did not show an alteration in the presence of SDM. Accordingly in sheep a parallel change in both the plasma protein binding and the tissue binding of TB might minimize any change in Vd as a function of plasma free fraction.

Since the Kp, f values did not show an alteration in the presence of SA except in the brain for all SAs, spleen for SP and SDM, and liver for SMZ (Table IV), the increase in $t_{1/2}$ by SA might be explained by the decrease in the hepatic intrinsic clearance (CL_{int}) (22). The tissue-to-plasma unbound concentration ratios (Kp, f) were not greater than one in any tissue studied (Table IV). The unusual tissue distribution of TB in rats may be attributed to several possible mechanisms, e.g., (a) the pH difference

between the intra- and extrahepatic fluids (33), (b) the existence of intracellular space which is impermeable to TB, and (c) heterogeneous TB distribution in the tissue.

The experimental observations in a previous paper (22) and in this study suggest that the physiologically based pharmacokinetic model shown in Fig. 1 can describe the distribution and elimination of TB in rats. In this study, good agreements were obtained between the predicted and observed time courses of TB concentrations in plasma and many tissues (Figs. 4 and 5). However, a disagreement of plasma concentration of TB was seen in the SMZ-treated rats, and this seemed to be due to an underestimation of the intrinsic clearance calculated using both the plasma protein binding and metabolic parameters obtained from *in vitro* studies (22). Another disagreement was seen between the observed and predicted TB concentrations in the brain (Fig. 5, panel c). When the plasma TB concentration increased, the apparent brain-to-plasma partition coefficients decreased (unpublished data), suggesting a plasma free concentration dependency of the TB distribution to the brain. This dependency, however, was not observed in the SP-treated rats. Previously, Spector and Lorenzo (34) suggested an active and saturable transport system from the cerebrospinal fluid to blood through the choroid plexus for weak acids such as salicylate, probenecid, and *p*-aminosalicyclic acid, which showed mutual transport inhibitions. Since TB and SA are also weak acids, similar mechanisms might affect the brain distribution of TB.

The release of insulin from β-cells might be induced by TB binding to the cell membrane (35), so the increase of unbound TB concentration in the pancreas may evoke insulin release from the β-cells, resulting in the depression of plasma glucose levels. Thus, it seems important to predict the time course of unbound TB concentration in the pancreatic vein, which is the primary determinant of TB binding to the β-cells. As shown in Fig. 6, the predicted unbound TB concentrations in the pancreatic vein at 6 h in the SP- and SDM-treated rats were six times higher than those of the control rats. Consequently, simulation based on the physiological pharmacokinetics may provide a good prediction of TB toxicity caused by TB–SP interaction reported in man (15).

In conclusion, the present study on the tissue distribution of TB in rats emphasizes the limitations of classical pharmacokinetic models in dealing with drug–drug interactions. In this study, we have developed a physiologically based pharmacokinetic model for the TB disposition in rats and demonstrated the potential application of this model to the prediction of the plasma and target organ drug concentrations in the presence of drug–drug interaction. This approach should also be very useful for developing insight into the mechanisms of drug–drug interaction.

ACKNOWLEDGMENT

The authors thank Dr. Ruichiro Nishigaki for his help in the lymph collection.

APPENDIX I: NOMENCLATURE

General

V	volume of tissue, ml
Q	blood flow rate through tissue, ml/min
C	tissue or blood concentration of tolbutamide, μg/ml
Kp	tissue-to-plasma partition coefficient of tolbutamide
Kp^B	tissue-to-blood partition coefficient of tolbutamide
Kp, f	tissue-to-plasma unbound concentration ratio of tolbutamide
s	plasma-to-blood concentration ratio of tolbutamide
f_p	plasma free fraction of tolbutamide
n	number of binding site
(p)	concentration of plasma protein, mM
K_d	dissociation constant of plasma protein binding, mM
v	oxidative metabolic rate of tolbutamide, μmol tolbutamide metabolized/min/12.4 g of liver
V_{max}	maximum velocity, μmol tolbutamide metabolized/min/12.4 g of liver
K_m	Michaelis constant, mM
λ	reciprocal of the injection time, min^{-1}

Subscripts

B	blood	Br	brain
P	plasma	Pa	pancreas
Li	liver	Sp	spleen
K	kidney	Ad	adipose
$G.I.$	gastrointestinal tract	Sk	skin
Lu	lung	Ar	arterial blood
H	heart	Ve	venous blood
M	muscle		

APPENDIX II: MODEL EQUATIONS

The following mass balance-blood flow equations describe the concentrations in each compartment of the pharmacokinetic model shown in Fig. 1.

Artery:

$$V_{Ar}\frac{dC_{Ar}}{dt}=(C_{Lu}/Kp^{B}_{Lu}-C_{Ar})Q_{Ar} \tag{12}$$

Vein:

$$V_{Ve}\frac{dC_{Ve}}{dt}=C_{Br}Q_{Br}/Kp^{B}_{Br}+C_{H}Q_{H}/Kp^{B}_{H}+C_{Li}Q_{Li}/Kp^{B}_{Li}+C_{K}Q_{K}/Kp^{B}_{K}$$
$$+C_{M}Q_{M}/Kp^{B}_{M}+C_{Sk}Q_{Sk}/Kp^{B}_{Sk}$$
$$+C_{Ad}Q_{Ad}/Kp^{B}_{Ad}-C_{Ve}Q_{Ve}+I(t) \tag{13}$$

where $I(t)$ is the injection function, which is a short pulse to simulate an intravenous injection as expressed by $I(t)=\text{dose}\ \lambda(\lambda t)^2\times(1-\lambda t)^2$; $\lambda=10\ \text{min}^{-1}$ (7).

Lung:

$$V_{Lu}\frac{dC_{Lu}}{dt}=(C_{Ve}-C_{Lu}/Kp^{B}_{Lu})Q_{Lu} \tag{14}$$

Liver:

$$V_{Li}\frac{dC_{Li}}{dt}=[(Q_{Li}-Q_{G.I.}-Q_{Pa}-Q_{Sp})C_{Ar}+C_{G.I.}Q_{G.I.}/Kp^{B}_{G.I.}$$
$$+C_{Sp}Q_{Sp}/Kp^{B}_{Sp}+C_{Pa}Q_{Pa}/Kp^{B}_{Pa}-C_{Li}Q_{Li}/Kp^{B}_{Li}]$$
$$-\frac{V_{\max}C_{Li}/Kp,f_{Li}}{K_m+C_{Li}/Kp,f_{Li}} \tag{15}$$

Noneliminating organ and tissue:

$$V_i\frac{dC_i}{dt}=(C_{Ar}-Ci/Kp^{B}_{i})Q_i \tag{16}$$

where i represents noneliminating organs or tissues, i.e., *Br*, *H*, *Pa*, *Sp*, *G.I.*, *K*, *M*, *Ad*, and *Sk*, respectively.

Tissue-to-blood partition coefficients (Kp^B) in Eqs. (12)–(16) were calculated as follows:

$$Kp^{B}_{j}=s\cdot f_p\cdot Kp,f_j \tag{17}$$

where j represents all tissues studied. Combining Eqs. (1) and (12) gives

$$Kp^{B}_{j}=\frac{s\cdot C_{p,f}\cdot Kp,f_j}{C_{p,f}+\dfrac{n(p)C_{p,f}}{K_d+C_{p,f}}} \tag{18}$$

Thus, substitution of Eq. (7) into Eq. (18) gives

$$Kp_j^B = s \cdot Kp, f_j/[1+n(p)/(K_d + C_j/Kp, f_j)] \tag{19}$$

REFERENCES

1. R. L. Dedrick and K. B. Bischoff. Pharmacokinetics in application of the artificial kidney. *Chem. Eng. Prog. Symp. Ser.* **64**:32–44 (1968).
2. H. S. G. Chen and J. F. Gross. Physiologically based pharmacokinetic models for anticancer drugs (general review). *Cancer Chemother. Pharmacol.* **2**:85–94 (1979).
3. K. J. Himmelstein and R. J. Lutz. A review of the application of physiologically based pharmacokinetic modeling. *J. Pharmacokin. Biopharm.* **7**:127–145 (1979).
4. N. Benowitz, R. P. Forsyth, K. L. Melmon, and M. Rowland. Lidocaine disposition kinetics in monkey and man I. Prediction by a perfusion model. *Clin. Pharmacol. Ther.* **16**:87–98 (1974).
5. N. Benowitz, R. P. Forsyth, K. L. Melmon, and M. Rowland. Lidocaine disposition kinetics in monkey and man II. Effects of hemorrhage and sympathomimetic drug administration. *Clin. Pharmacol. Ther.* **16**:99–109 (1974).
6. L. I. Harrison and M. Gibaldi. Physiologically based pharmacokinetic model for digoxin disposition in dogs and its preliminary application to humans. *J. Pharm. Sci.* **66**:1679–1683 (1977).
7. K. B. Bischoff and R. L. Dedrick. Thiopental pharmacokinetics. *J. Pharm. Sci.* **57**:1346–1351 (1968).
8. K. B. Bischoff, R. L. Dedrick, D. S. Zaharko, and J. A. Longstreth. Methotrexate pharmacokinetics. *J. Pharm. Sci.* **60**:1128–1133 (1971).
9. R. L. Dedrick, D. D. Forrester, J. N. Cannon, S. M. E. Dareer, and L. B. Mellett. Pharmacokinetics of 1-β-arabinofuranosylcytosine (ARA-C) deamination in several species. *Biochem. Pharmacol.* **22**:2405–2417 (1973).
10. B. Montadon, R. J. Roberts, and L. J. Fischer. Computer simulation of sulfobromophthalein kinetics in the rat using flow-limited models with extrapolation to man. *J. Pharmacokin. Biopharm.* **3**:277–290 (1975).
11. P. A. Harris and J. F. Gross. Preliminary pharmacokinetic model for adriamycin (NSC-123127). *Cancer Chemother. Rep.* Part I, **59**:819–825 (1975).
12. L. I. Harrison and M. Gibaldi. Physiologically based pharmacokinetic model for digoxin distribution and elimination in the rat. *J. Pharm. Sci.* **66**:1138–1142 (1977).
13. R. H. Smith, D. H. Hunt, A. B. Seifen, A. Ferrari, and D. S. Thompson. Pharmacokinetic model for procaine in humans during and following intravenous infusion. *J. Pharm. Sci.* **68**:1016–1024 (1979).
14. R. H. Luecke and W. D. Wosilait. Drug elimination interactions: analysis using a mathematical model. *J. Pharmacokin. Biopharm.* **7**:629–641 (1979).
15. E. Schulz and F. H. Schmidt. Abbauhemmung von tolbutamid durch sulfaphenazol beim menschen. *Pharmacol. Clin.* **2**:150–154 (1970).
16. M. Kristensen and L. K. Christensen. Drug induced changes of the blood glucose lowering effect of oral hypoglycemic agents. In C. A. Loubatieres and A. E. Rengold (eds.), *Pharmacology and Mode of Oral Hypoglycemic Agents*, Vol. VI. Casea Editrice "Li Ponte", Milano, 1969 pp. 116–136.
17. M. Rowland and S. B. Matin. Kinetics of drug–drug interactions. *J. Pharmacokin. Biopharm.* **1**:553–567 (1973).
18. S. M. Pond, D. J. Birkett, and D. N. Wade. Mechanisms of inhibition of tolbutamide metabolism: phenylbutazone, oxyphenbutazone, sulfaphenazole. *Clin. Pharmacol. Ther.* **22**:573–579 (1977).
19. J. Shibasaki, R. Konishi, and K. Yamasaki. Tolbutamide-sulfaphenazole interaction in rabbits. *J. Pharmacokin. Biopharm.* **5**:277–290 (1977).

20. J. J. Thiessen and M. Rowland. Kinetics of drug–drug interactions in sheep; tolbutamide and sulfadimethoxine. **66:**1063–1070 (1977).
21. Y. J. Lin, S. Awazu, and M. Hanano. Inhibitory mechanism of sulfaphenazole on tolbutamide elimination from plasma in rats. *J. Pharm. Dyn.* **2:**273–285 (1979).
22. O. Sugita, Y. Sawada, Y. Sugiyama,. T. Iga, and M. Hanano. Prediction of drug–drug interaction from *in vitro* plasma protein binding and metabolism. A study of tolbutamide-sulfonamides interaction in rats. *Biochem. Pharmacol.* **30:**3347–3354 (1981).
23. M. Hanano. Library program (D_2/TC/RKM) of the University of Tokyo Computer Center, Tokyo, Japan (1980).
24. R. L. Dedrick. Animal scale-up. *J. Pharmacokin. Biopharm.* **1:**435–461 (1973).
25. Y. Sasaki and H. N. Wagner. Measurement of the distribution of cardiac output in unanesthetized rats. *J. Appl. Physiol.* **30:**879–884 (1971).
26. R. L. Dedrick, D. S. Zaharko, and R. J. Lutz. Transport and binding of methotrexate *in vivo*. *J. Pharm. Sci.* **62:**882–890 (1973).
27. R. J. Lutz, R. L. Dedrick, H. B. Matthews, T. E. Eling, and M. W. Anderson. A preliminary pharmacokinetic model for several chlorinated biphenyls in the rat. *Drug Metab. Dispos.* **5:**386–396 (1977).
28. H. S. G. Chen and J. F. Gross. Estimation of tissue-to-plasma partition coefficients used in physiological pharmacokinetic models. *J. Pharmacokin. Biopharm.* **7:**117–125 (1979).
29. J. R. Gillette. In *Handbook of Experimental Pharmacology, Vol. 28, Concepts in Biochemical Pharmacology*, Part 3. chap. 60, Springer-Verlag, Berlin, 1975, Chap. 60, pp. 35–85.
30. H. Y. Yu, Y. Sawada, Y. Sugiyama, T. Iga, and M. Hanano. Effect of sulfadimethoxine on thiopental distribution and elimination in rats. *J. Pharm. Sci.* **70:**323–326 (1981).
31. B. Fichtl, H. Kurz, I. Wachter, and A., Ziegler. Binding of drugs to muscle tissue: drug interactions. *Naunyn-Schmideberg's Arch. Pharmacol.* **302:**R2 (1978).
32. W. M. Wardell. Drug displacement from protein binding: source of the sulphadoxine liberated by phenylbutazone. *Br. J. Pharmacol.* **43:**325–334 (1971).
33. A. Roos and W. F. Boron. Intracellular pH. *Physiol. Rev.* **61:**296–434 (1981).
34. R. Spector and A. V. Lorenzo. The effects of salicylate and probenecid on the cerebrospinal fluid transport of penicillin, aminosalicyclic acid and iodide. *J. Pharmacol. Exp. Ther.* **183:**55–65 (1974).
35. J. Sehlin. Evidence of specific binding of tolbutamide of the plasma of pancreatic β-cells. *Acta Disbetol. Lat.* **10:**1052–1060 (1973).